Received: 10 March 2014, Revised: 9 April 2014, Accepted: 10 April 2014, Published online in Wiley Online Library:

(wileyonlinelibrary.com) DOI: 10.1002/env.2280

Scenarios for future wildfire risk in California: links between changing demography, land use, climate, and wildfire

Benjamin P. Bryant[a] and Anthony L. Westerling[b]*

Over 21,000 future California residential wildfire risk scenarios were developed on a monthly 1/8° grid, using statistical wildfire models. We explore interactions between two global emissions scenarios, three climate models, six spatially explicit population growth scenarios derived from two growth models, and a range of parameters defining properties' vulnerability to loss. Scenarios are evaluated over two future time periods relative to historic baselines. We also explore effects of spatial resolutions for calculating household exposure to wildfire on changes in estimated future property losses. Our goal was not to produce one authoritative set of future risk scenarios but rather to understand what parameters are important for robustly characterizing effects of climate and growth on future residential property risks. By end of century, variation across development scenarios accounts for far more variability in statewide residential wildfire risks than does variation across climate scenarios. However, the most extreme increases in residential fire risks result from combining high-growth/high-sprawl scenarios with the most extreme climates considered here. Case studies for the Bay Area and the Sierra foothills demonstrate that, while land use decisions profoundly influence future residential wildfire risks, effects of diverse growth and land use strategies vary greatly around the state.

Additional supporting information may be found in the online version of this article at the publisher's web site.

Keywords: fire; wildfire; risk; climate; scenario; WUI; wildland–urban interface; spatial

1. INTRODUCTION

1.1. Climate change and residential wildfire risk

Wildfires in California routinely threaten people and property, destroy homes, force evacuations, expose large populations to unhealthful air, and result in deaths and injuries. Climate change may affect the size and frequency of wildfires in California, and its impacts are likely to vary substantially across the state (Westerling *et al*. 2011a; Bowman *et al*. 2009; Krawchuk *et al*. 2009; Westerling and Bryant 2008; Westerling *et al*. 2006; and Lenihan *et al*. 2003). And while wildfire poses many hazards, its most direct impacts on humans are fundamentally connected to how people are distributed over the landscape. In previous work (Bryant and Westerling 2009), we considered how changes in the probability of large fire events interact with changes in land use to affect residential property risks, drawing on a small number of scenarios for future climate, land use, and growth. In this paper, we expand the number of climate, land use, and growth scenarios considered and also consider additional uncertainties and a more sophisticated model of expected housing loss due to wildfire, to more robustly characterize future changes in wildfire and wildfire-related residential property risk in California. A complementary study (Hurteau *et al*. 2014) applies our results to assess changes in wildfire emissions of greenhouse gases and air pollutants.

This paper's primary aim is to describe how climate change and human development patterns over California may interact to lead to differing levels of fire-caused risk to residential property, with a greater focus on the relative impacts of different climate, population growth, and land use scenarios, as well as parameters related to fire management. This study used climate scenarios derived from three global climate models (GCMs) from the Intergovernmental Panel on Climate Change (IPCC)'s Fourth Assessment forced with medium-high and low emissions pathways (Special Report on Emissions Scenarios (SRES) A2 and B1, respectively) (IPCC 2000, 2007). Our growth scenarios are derived from two different sets of spatially explicit raster data sets, each describing different 21st century population growth and land use scenarios. One set is based on work by Theobald (2005) and developed by the US Environmental Protection Agency (US EPA 2008) as the Integrated Climate and Land Use Scenarios (ICLUS) for the USA and is provided at 100 m resolution. The other set is provided at 50 m resolution and generated using the UPlan growth model, developed for California by Thorne *et al*. (2012). As in Bryant and Westerling (2009), the primary results of this study are in the form of statistics on aggregate statewide relative risk, where the reference period is defined based on year 2000 development patterns and late 20th century (1961–1990) simulated climate. This paper also presents spatial distributions of changes in wildfire probabilities and expected losses to illustrate how these impacts can vary throughout the state.

* *Correspondence to: A. L. Westerling, Sierra Nevada Research Institute, University of California, Merced, CA 95343, U.S.A. E-mail:awesterilng@ucmerced.edu*

a *Pardee RAND Graduate School, the RAND Corporation, Santa Monica, U.S.A.*

b *Sierra Nevada Research Institute, University of California, Merced, U.S.A.*

In the remainder of the paper, we first review some impacts of wildfires. In Section 2, we develop our conceptual model and describe the data we have available for implementing such a model. Section 3 summarizes the content of the online supplement, in which we build up a formal model for estimating changes in wildfire risk, in the process clarifying our assumptions and how we handle the significant uncertainties inherent in considering long-term scenarios of such risk. Section 4 discusses the study's primary findings, including changes in aggregate statewide risk and also some subregional analysis, while Section 5 summarizes the results and considers their policy implications.

1.2. The ecological context of human interactions with fire

While this work focuses on risks to residential property, there are many other less-obvious impacts, both to humans and also to ecosystems, some of which are listed in Table 1. (See the California Board of Forestry's California Fire Plan [1996] for a thorough assessment of wildfire impacts). This paper focuses only on quantifying changes in direct damages to homes; therefore, when evaluating this study's results, it is important to remember that these impacts represent just a fraction of the total impacts from wildfire. While monetization of many of the impacts listed in Table 1 is difficult and fraught with uncertainty, the California Department of Forestry estimated that, for example, watershed impacts of wildfire, in the form of soil erosion and potential required sediment removal from water bodies, may easily average out to magnitudes on the order $100 per acre burned, possibly even up to thousands of dollars per acres burned in some cases (California Board of Forestry, 1996). This translates to at least tens of millions of dollars of annual impacts currently from that source alone. In addition, many of the environmental impacts have human consequences. The health and viewshed impacts of reduced air quality are readily apparent, but there are other more subtle and second-order effects, such as watershed impacts reducing desired fish populations and reducing power generation ability from hydroelectric dams.

When considering damages, it is important to acknowledge that wildfire is in principle a natural phenomenon that serves a role in maintaining healthy ecosystems, but human presence and action combine to make fire both a risk to humans, and also potentially a risk to ecosystems. This is due to humans causing unnatural *patterns* of wildfire with intensities or frequencies outside the range of natural variability (Dellasala *et al*. 2004). For example, Stephens *et al*. (2007) estimate that fire suppression and land use changes reduced annual burned area in California forests from presettlement levels by more than 90 percent in the 20th century. This long-term exclusion of wildfire may have led to increases in biomass and changes in fuel structure in some California forests that in turn have fostered hotter, more-intense forest wildfires that are harder to manage and may have had undesirable effects in forest ecosystems that are not adapted to high-severity fire (Gruell 2001; Allen *et al*. 2002; Miller *et al*. 2009). For another example, wildfire in chaparral ecosystems may not have been significantly affected by fire suppression, but pressures from increased development and human ignitions may have increased wildfire frequency and fostered invasion by exotic species (Keeley and Fotheringham 2003; Syphard *et al*. 2007). These changes can affect ecosystems in undesirable ways that may or may not be proportional to the residential impacts addressed here. With the importance of these ecological considerations in mind, we now turn to our focus on the risk of housing destruction due to wildfires.

2. CONCEPTUAL MODEL OF LONG-RANGE WILDFIRE RISK AND AVAILABLE SCENARIO DATA

Climate change impacts wildfire characteristics, as does human development on the landscape. In turn, changes in wildfire characteristics affect the risk posed to that same human development. This section outlines these interactions at a conceptual level and discusses historical and modeled data available to us for considering different futures in a more quantitative way. The following section then formalizes these considerations into a quantitative risk model, in which risk is framed as expected losses of residential housing units to wildfire.

2.1. Conceptual linkages between growth, fire, and risk

On seasonal to interannual timescales, climate-fire relationships describe the response of existing ecosystems to climate variability that affects fuel availability and flammability, with the relative importance of each varying significantly with ecosystem characteristics (e.g., Westerling *et al*. 2003; Girardin *et al*. 2009; Littell *et al*. 2009; Westerling 2010; Krawchuk and Moritz 2011). Climatic effects that influence the availability of fine surface fuels (grasses, forbs) tend to dominate in dry, sparsely vegetated ecosystems, while effects on flammability tend to dominate in moister, more densely vegetated ecosystems, although there is often not a clear partition between the two effects (Westerling *et al*. 2003; Littell *et al*. 2009; Westerling 2010; Krawchuk and Moritz 2011). On decadal timescales, shifts in climate that affect the spatial ranges of vegetation assemblages, and/or their productivity, have the potential to qualitatively alter fire regime responses to shorter-term climate variability.

Table 1. Types of wildfire impacts

Direct human impacts	Indirect impacts
Structures burned/property value lost	Watersheds-soil loss, deposits
Prevention and suppression expenditures	Timber loss
Evacuation costs/lost productivity	Habitat disruption
Lives lost and adverse health effects of smoke	Species loss
Diminished recreational opportunities and viewsheds	Nonnative species invasion
Disruption to infrastructure availability	

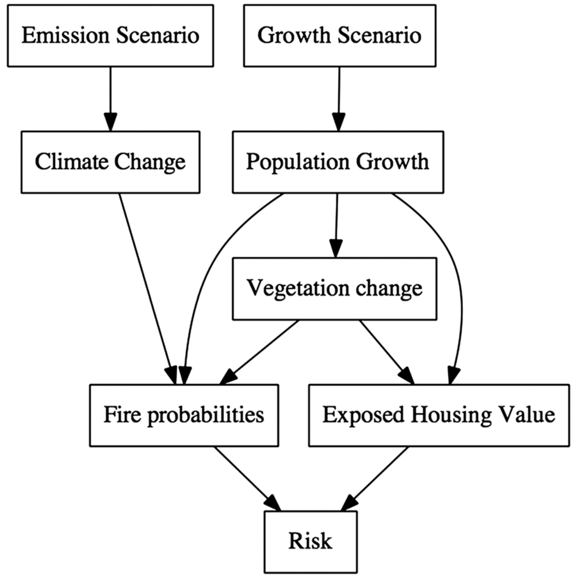

Figure 1. Conceptual model of how climate change and growth affect long-term fire risk

In this study, the statistical fire models used allow a focus on how fire in existing ecosystems may respond to climate change, while the ecosystems themselves and their fire-climate relationships are implicitly assumed to remain fixed (as in Westerling *et al.* 2011a). To the extent that projected changes in climate and the resulting disturbance regimes may lead to qualitative changes in ecosystem responses to climate variability, these models may exhibit potentially significant biases, particularly for the warmest, driest scenarios toward the end of the century.

As with climate, vegetation, and their attendant fire patterns, the distribution of people over the landscape also changes with time and impacts eventual expected losses due to fires (fire risk). In fact, all of these changes are potentially interlinked, although some links are stronger than others. Furthermore, changes in one variable may increase risk through one link while decreasing it through another. As an example of this phenomenon, development in a given region decreases the vegetation footprint available for the ignition of wildfires, but human presence may more than compensate by an increase in human-caused ignitions. However, the increased presence of humans may sometimes decrease fire size in the region, through early identification of fires and increased suppression efforts.[1] In general, the statistical relationship between population density and the human-related "risk of fire" is some form of inverted U (or even one having multiple maxima), with zero humans to be exposed to wildfire at zero population density, and zero wildfire at some saturated density (at an appropriately defined spatial scale), where everything is urban and *wild*fires cannot exist (Guyette *et al.* 2002). However, the range of shapes possible in between these extremes in our study area is not known and likely highly contingent on many other variables associated with the locality.

To capture this dynamic and others, our model of fire risk accounts for human impacts on wildfire probabilities and also allows for human development to act in ways that mitigate their exposure to fire proportionally with the value at risk, where *exposure* describes the expected losses entailed by the occurrence of a fire event. These relationships are shown conceptually above (Figure 1). Global growth scenarios affect emissions that drive climate change. Local growth scenarios, which are not necessarily coupled to global growth patterns, generate spatially explicit population trajectories through time. As modeled by Westerling *et al.* (2011a), this population distribution, together with climate change, affects wildfire occurrence and burned area, both directly and through their joint impact on vegetation change (S.1).

However, understanding changes in wildfire risk in terms of the potential loss of homes require additional information beyond fire probabilities and burned areas: It requires an estimate of how those spatially explicit fire patterns interact with spatially explicit changes in housing across the state. Large increases in fire occurrence where there are no homes do not increase risk of housing loss, while new growth in a fire-prone area may dramatically increase risk even under unchanging fire behavior. Therefore, the focus of the present paper is on transforming scenarios of spatially explicit population growth into estimates of value exposed to loss from wildfire and then linking those exposed value estimates with fire probabilities to generate estimates of overall risk.

We next present the data available to us for this task. Our treatment of the data specific to estimating fire probabilities is highly condensed, because there are many data sources (these are summarized graphically in Figure S.2, which follows the detailed model description), and their use in generating fire probabilities and burned area has been described elsewhere, such as in Westerling *et al.* (2011a).

[1]The relationships between human presence, ignitions, and fire size are quite complex. The fire history data used here indicate that most large fires in coastal southern California are ignited by human activities; whereas, lightning ignitions play a more important role in Northern California forests. The large populations in coastal southern California and other areas of the state adjacent or easily accessible to urban population centers may imply a saturation of potential ignition sources in many parts of the state in recent decades (see Guyette et al. 2002). At the same time, only large fires (>200 ha) are modeled here. The vast majority of wildfires reported in the state are below that threshold and excluded from analysis, while the vast majority of burned area is accounted for by the largest fires. Climate exerts a strong influence on whether ignitions—human or natural—can spread into fires larger than 200 ha. Consequently, the number of large fires may not be as sensitive to variability in human ignitions as it is to other factors, including climate. More difficult issues for predicting burned area accurately are clustering in lightning ignitions in northern California, such as in 1987 and 2008, and high wind events that fatten the extreme tail of the fire size distribution but may not significantly affect the number of ignitions.

2.2. Summary of nongrowth scenario data used in the fire probability model

2.2.1. Historical climatic, hydrologic, and land surface characteristics data

A common set of historical climate data, including gridded maximum and minimum temperature and precipitation and simulated hydrologic data, were assembled by the California Climate Change Center at the Scripps Institution of Oceanography for the 2006 California Scenarios project and the subsequent California Vulnerability and Adaptation project. Gridded daily climate data (temperature and precipitation) derived from historical (1950–1999) station observations were obtained online from Santa Clara University (see Maurer *et al*. 2002; Hamlet and Lettenmaier 2005; http://www.engr.scu.edu/~emaurer/data.shtml). Westerling *et al*. (2011a) then used these data with wind speed, topographic, and vegetation data to force the Variable Infiltration Capacity (VIC) macroscale hydrologic model at a daily time step in full energy mode with climatologic winds, producing hydroclimatic variables such as actual evapotranspiration, surface temperature, and snow water equivalent (Liang *et al*. 1994). The VIC model solves for water and energy balances given daily temperature, precipitation, and wind speed values as inputs. Westerling *et al*. (2011a) used the Penman–Monteith equation to estimate potential evapotranspiration (Penman 1948; Monteith 1965) and then calculated moisture deficit (potential minus actual evapotranspiration).

For the VIC inputs, Westerling *et al*. (2011a) used coarse vegetation categories based on the University of Maryland vegetation classification scheme with fractional vegetation adjustment (Hansen *et al*. 2000) and topographic data on a 1/8-degree grid obtained from the North American Land Data Assimilation System (LDAS, see Mitchell *et al*. 2004; accessed online at http://ldas.gsfc.nasa.gov/). The LDAS topographic layers are derived from the GTOPO30 Global 30 Arc Second (~1 km) Elevation Data Set (Gesch and Larson 1996; Verdin and Greenlee 1996; Mitchell *et al*. 2004). The LDAS data also provided inputs for the (Westerling *et al*. 2011a) fire models used in this study, including gridded aspect and vegetation fractions. Wind speed data for 1950–1999 were accessed online from the National Centers for Environmental Prediction Reanalysis project (http://www.esrl.noaa.gov/psd/data/reanalysis/) and used to calculate a monthly wind speed climatology interpolated to the LDAS grid for use in the VIC hydrologic simulations. Relative humidity and shortwave radiation values used in VIC were derived from the MT-CLIM algorithm, version 4.2, using temperature and precipitation as inputs (see Kimball *et al*. 1997; Thornton and Running 1999; Pierce et al 2013).

2.2.2. Projected climate and hydrologic data

Cayan *et al*. (2009) obtained and downscaled 12 future climate scenarios for the California Vulnerability and Adaptation project and used temperature and precipitation from these scenarios to force VIC hydrologic simulations, as described for the historical data mentioned earlier. A subset of six of those future climate scenarios are used here, derived from three GCMs (National Center for Atmospheric Research [NCAR] PCM 1, Centre National de Recherches Météorologiques [CNRM] CM 3.0, and Geophysical Fluid Dynamics Laboratory [GFDL] CM 2.1) from the IPCC's Fourth Assessment (AR4), forced with medium-high and low emissions pathways (the SRES A2 and SRES B1scenarios). These scenarios were downscaled by Cayan *et al*. (2009) using the bias-corrected constructed analogs method (Maurer *et al*. 2010.)

While the PCM 1 model from NCAR is an older-generation model that is not as up to date as the others, it was included because it is an outlier among the IPCC models, with lower climate sensitivity and smaller temperature increases over California than most other models. The CNRM and GFDL model sensitivities span the middle of the range of temperature projections available for California, but not the warmest scenarios that have been projected for the region. The NCAR model used here tends to have insignificant changes in precipitation over California by end of century, while the GFDL and CNRM models tend to project decreased precipitation (Cayan *et al*. 2009). Even where precipitation does not change significantly, increased temperatures can lead to drier fuels through increased evaporation and transpiration. Thus, the scenarios used here span the lower to intermediate range projections for warmer, mostly drier conditions over California.

2.2.3. Fire history data

While fire ignitions may be plentiful, most wildfires are too small to be consequential. Typically, a small fraction of all fires generates the vast majority of the total area burned, suppression costs, and damages (e.g., Strauss *et al*. 1989; Johnson 1992; Strategic Issues Panel on Fire Suppression Costs 2004). Documentary records of larger fires also tend to be more comprehensive and higher quality, probably because of their greater economic and ecological consequences, and focusing on the small subset of large fires results in data that are more tractable to quality assurance efforts (Westerling *et al*. 2006). Therefore, we restrict our analysis to fires exceeding 200 ha in size.[2]

Westerling *et al*. (2011a) used fire history (1980–1999) data to estimate the fire models employed here and described in Section 3.2. Their data are an extension and update of the data sets used in Westerling *et al*. (2006), with the data methodology described in the online supplementary materials to Westerling *et al*. (2006). The portion of their fire history used here incorporates documentary records from the California Department of Forestry and Fire Protection (CalFire), county fire departments under contract with CalFire, US Department of Interior agencies (Bureau of Land Management, Bureau of Indian Affairs, and National Park Service), and the US Department of Agriculture (Forest Service) to produce a comprehensive record of large fires covering most of the state and federal protection responsibility areas in California.[3] These are for wildfires that were classified as "action" or "suppression" fires, as opposed to prescribed or natural fires used to meet vegetation management goals. These data were aggregated by month on a 1/8-degree latitude and longitude grid, producing numbers of large fires and

[2]The arbitrary 200 ha threshold was selected for historical reasons: The Canadian Large Fire History uses a 200 ha threshold (Stocks et al. 2002), so a consistent threshold was used to facilitate creation of a western North American fire history. This threshold allows the creation of a comprehensive data set that captures most of the burned area in the region and meets statistical requirements for selecting a threshold value for estimating generalized Pareto distributions (Holmes et al. 2008).

[3]Local responsibility areas (LRAs) were excluded. LRAs are mostly urban and agricultural areas that account for most of the population of the state, but very few of its large wildfires.

total area burned in those fires by the month and grid cell in which the fires were reported to have ignited. The fire probabilities simulated here reflect associations with historical climate and land surface characteristics detected in these historical fire data for California.

2.3. Spatially explicit population growth scenarios

We use two sources of spatially explicit housing scenarios as inputs to several variables in our model and increase the richness of our explorations by considering variations derived from each source. In both cases, the primary data source provides fine-resolution raster data, where each raster cell holds an expected housing density and an expected population per housing unit. We then use these data sources as inputs into the following:

1. population for the fire probability model;
2. vegetation fractions used in both the fire probability model and the exposure model;
3. initial vulnerable values in the exposure model.

S7–S9 describe our algorithmic transformations of the data to extract the aforementioned model inputs from the raw scenario data. Here, we simply describe the data sources as they relate to our scenario modeling.

2.3.1. Integrated climate and land use scenarios

The ICLUS were developed to create thematically consistent land-use scenarios at high resolution across the USA (US EPA 2008). They link country-level population growth assumptions with the Spatially Explicit Regional Growth Model developed by Theobald (2005) to generate housing density projections at the 100 m level through the end of the 21st century. The ICLUS scenarios used for this study provide three different growth trajectories, originally intended to correspond with the SRES scenarios: A2 referred to a higher growth scenario relative to a base case scenario (with a higher population growth and higher population per housing unit), and B1 referred to a lower growth population scenario. Because there need not be a strict correlation between the growth path of California and the global population storyline driving global climate, we vary these scenarios independently, and henceforth refer to ICLUS B1, base case, and A2 scenarios as “low” “mid” and “high” to avoid confusion with the climate-specific scenarios, which we still refer to by their SRES labels of B1 and A2.

These projections were provided on a 100 m raster (where each cell is a “tract” as described in Section 3.1, and in contrast with the much larger 1/8 degree “grid cell”). Because of the sensitivity of our model to the density of tracts, and in turn the sensitivity of the density to the scale at which density is defined,[4] we also aggregate the ICLUS data to higher levels—to cells with 200, 400, and 800 m sides—and perform our loss calculations for each case.

2.3.2. UPlan growth scenarios for California

The UPlan scenarios were developed specifically for California by Thorne *et al*. (2012) and offer a set of projections for how new growth is distributed spatially throughout California in the year 2050, with the same amount of population growth in each scenario. They have numerous strengths relative to ICLUS but also possess some key drawbacks specific to modeling fire risk. Like ICLUS, they offer three growth scenarios,[5] although unlike ICLUS they are not explicitly or conceptually tied to the SRES scenarios. One scenario is a business-as-usual case (“bau”), another refers to smart growth (“smart”), and another is premised on reducing development in areas assigned moderate or higher fire hazard severity ratings by CalFire (“fire”). It should be noted, however, that the fire hazard severity ratings are rather distinct from the risk measures generated here in that they account for fuel characteristics directly and are generally provided at a far finer spatial scale. Different hazard zones vary down to a minimum of 8 ha in size for urban areas and 80 ha for wildland areas. By contrast, one grid cell in our model is on the order of 14400 ha. These discrepancies may contribute to some of the nonintuitive results that are seen when comparing UPlan scenarios later on.

The UPlan data has a finer spatial resolution (50 m) compared to ICLUS, but the drawback of a coarser-density resolution, allowing new growth to occur in only a small number of discrete density classes (such as one housing unit per acre, five housing units per acre, and so on). Unlike the version of ICLUS we rely on, UPlan also has the advantage of explicitly projecting the future footprint of commercial and industrial growth and also allotting all new growth based on attractors that include actual county zoning plans. Unfortunately, while UPlan may better represent the processes of future growth, the drawback is that it does not rely on any explicit representation of the base year housing distribution, beyond assuming an urban mask in which new growth does not occur. This creates challenges when attempting to make valid risk estimates relative to a base year, which is addressed in S.7.

3. FORMALIZING AND IMPLEMENTING THE RESIDENTIAL WILDFIRE RISK MODEL

This section establishes an expected loss framework of wildfire risk that ties together fire probabilities and expected losses contingent on fire events and discusses how we created the computational experimental design that specified our many thousands of scenarios. The online

[4]As an example to illustrate the importance of spatial scale, consider an urban threshold of 10 households per hectare, and a 200 m× 200 m cell, which is subdivided into four 100 m× 100 m cells. If three of the 100 m—scale cells contain nine households and one cell contains 17, one arrives at very different outcomes dependent on the spatial scale: Using the 100 m spatial scale, three cells would be vulnerable, and one would be considered urban; whereas, at the 200 m scale, the average density would be 11, and therefore, all 4 ha would be considered urban.

[5]The study used scenarios and related spatial data made available in mid-2011. Additional scenarios have since been developed, as described in Thorne et al. (2012).

supplement details how we addressed the challenges of modeling expected losses when the joint spatial distribution of housing development and vegetation landscape cannot be predicted with any meaningful certainty—particularly at the fine spatial scales of our growth data; see the online Supplement. It includes a discussion of the many cross-linkages between climate, growth, fire, and exposure to wildfire risk, and how our model links many data sources and intermediate data products to produce our ultimate risk estimates. By contrast, this section extracts the minimum information necessary to interpret our scenarios and results.

3.1. A nested model of residential wildfire risk

We focus first on the overall model of expected losses due to wildfire within a grid cell R, which is composed of tracts of equal area that together partition R.[6] In this modeling effort, the region R is a 1/8-degree grid cell mentioned earlier, and each tract is a raster cell as provided by either ICLUS or UPlan scenarios. Each region R is therefore approximately a rectangle with sides of 10–14 km, and each tract is a square with sides between 50 and 400 m (depending on the data source and parameter settings). Each tract τ_i ($i \in 1..N_\tau$) contains some value V_i, where *value* may be defined as monetary value, or, with increasing coarseness, the number of housing units or structures. Our analysis assumes that value is described by number of housing units, because that is how our growth scenario data was provided. To avoid spurious reliance on the very fine-grained detail provided by the growth scenarios, the study does not assume exact knowledge of the spatial distribution of housing units within each cell but instead uses that detailed information to create frequency distributions of tract values for each grid cell.

Following prior work (Preisler and Westerling 2007 and Westerling and Bryant 2008; Preisler *et al*. 2011; Westerling *et al*. 2011a; and Westerling *et al*., 2011b), we model a grid cell R as having a time-varying probability $P(F)$ of large fire occurrence, assumed to be a function $f_P(POP, VEG, C)$ of the population within the region (POP), fraction of the region that is vegetated (VEG), and other variables C, such as hydroclimate and diverse land surface characteristics. (Each of these sets of variables includes time-varying elements, but for notational simplicity, we do not include time subscripts.) Any specific fire is associated with a perimeter that encompasses some subset of the tracts within R. And while the spatially explicit distribution of fire events is difficult to estimate, each tract can be considered to have some baseline probability of being encompassed by fire, conditional on a fire event within the region.[7] We denote this $P(\tau_i \in \tau_F|F)$, where τ_F denotes the set of tracts encompassed by a fire. Then, by breaking out conditional probabilities, we can express the total expected loss within R as

$$E(LOSS) = f_P(POP, VEG, C) \times \sum_{i=1}^{N_\tau} [P(\tau_i \in \tau_F|F) \times (L(V_i)|\tau_i \in \tau_F)] \quad (1)$$

This says that the expected loss in R is the probability of a fire within R multiplied by the sum of expected losses in each tract, given that there is a fire in R. The expected loss in each tract is similarly decomposed into the probability of that tract falling within a fire perimeter and the expected loss $L(V_i)$ contingent on a tract falling within a fire perimeter. We refer to this approach as *nested* because it identifies expected losses within each region by considering expected losses within each tract, contingent on a fire event. While "grid cell level conditional expected losses" would perhaps be the most accurate term to describe this latter concept, we refer to the right half of Equation (1) as "exposure" or "exposed value." It is slightly at odds with some other definitions of exposure, but consistent with the idea that exposed value is what will be lost in the event of the main hazard (wildfire in the region) coming to pass.

While theoretically consistent, we do not necessarily have historical or modeled data to support identifying every element of the aforementioned equation. The next section discusses each component of the aforementioned equation and the strategies used to estimate changes in risk while accounting for the uncertainty and data limitations.

3.2. Fire probability model

This study used the logistic regression models and data (summarized in Sections 2.2.1–2.2.3) of Westerling *et al*. (2011a) to estimate monthly probabilities of fires in state and federal protection responsibility areas in California that exceed 200 and 8500 ha occurring in a region R. These probabilities are described as functions of climate, simulated hydrology, land surface characteristics, population, and growth footprint; R is a cell on a 1/8 degree latitude/longitude grid (see also Preisler *et al*. 2004). Area burned in these fires is estimated using generalized Pareto distributions (GPDs) fit to fires between 200 and 8500 ha and to fires >8500 ha, assuming that the fire size distributions are stationary over time and space. Monthly estimates produced are then averaged over time periods 1961–1990, 2035–2064, and 2070–2099 to produce expected annual fires and expected annual areas burned for each region within those periods.

Formally, the probability of a fire greater than 200 ha occurring in region R for a given month, denoted $P(F)$, is estimated using a logistic regression model of the form:

[6]The equal area assumption is not necessary to implement our approach, but essentially holds true for our raster-based growth scenario data and simplifies presentation and implementation of the method.
[7]While somewhat cumbersome, we generally use the terminology of a tract "falling within a fire perimeter" rather than the far shorter "burning." This is in recognition of the fact that modern fire protection approaches mean that sometimes housing structures may be encompassed within a fire perimeter, but not actually burn, due to the successful creation of defensible space and appropriate construction techniques, among other factors. Our terminology is therefore a conceptual distinction and also one that is formally represented in our model.

$$\begin{aligned} Logit(P(F)) &= \log(P/(1–P)) \\ &= \boldsymbol{\beta} \times [1, D30, D01, D02, PCP, G(D30, AET30), \\ &\quad G(D30, AET30) \times TMP, G(D30, AET30) \times CD0, \\ &\quad G(TMP), G(RH)\ G(POP), G(POP) \times D30, G(VEG), FRA\ ] \end{aligned} \tag{2}$$

where

β is a vector of parameters estimated from the data,
[*] is a matrix of explanatory variables,
G() are matrices describing semi-parametric smooth transformations of the data as described in Preisler and Westerling (2007),

G(*D*30,*AET*30) is a thin-plate spine that estimates a spatial surface as a function of 30-year (1961-1990) average cumulative October–September moisture deficit (*D*30) and actual evapotranspiration (*AET*30) (Preisler and Westerling 2007; Preisler *et al*. 2011); we relied on modules for fitting thin-plate splines within R provided by the Geophysical Statistical Project (http://www.cgd.ucar.edu/stats/Software/Fields) that serves as a proxy for coarse vegetation characteristics (Westerling *et al*. 2011a online supplement),

*D*01 and *D*02 are the 1-year and 2-year leading cumulative October–September moisture deficit,
*CD*0 is the cumulative from October to current month moisture deficit,
PCP is the 2-month cumulative precipitation through the current month,
G(*TMP*) is the second-order polynomial transformation of monthly average surface air temperature,
G(*RH*) is the second-order polynomial transformation of $RH = log((x + 0.002)/(1 - x + 0.002))$, where x is monthly average relative humidity,
G(*VEG*) is a degree 3 basis spline transformation of $VEG = log((x + 0.002)/(1 - x + 0.002))$, where x is the vegetation fraction,
G(*POP*) is the second-order polynomial transformation of total population,
and *FRA* is $log((x + 0.002)/(1 - x + 0.002))$ where x is federal protection responsibility area as a fraction of total area.

The expected area burned, given that a fire greater than 200 ha occurs, is

$$\begin{aligned} E(A(F)) = (1 - P(F|A(F) > 8500))*E(A(F) \mid A(F) < 8500))+ \\ P(F|A(F) > 8500)*E(A(F) \mid A(F) > 8500)) \end{aligned}$$

where $E(A(F)|A(F) < 8500))$ is the expected area burned by fires in the range from 200 to 8500 ha, conditional on a fire greater than 200 ha occurring in the grid cell. This area is estimated from a truncated GPD fit to historical fires observed in California. Similarly,
$E(A(F)|A(F) > 8500))$ is the expected area burned given that at least 8500 ha burned, and $P(F|A(F) > 8500)$ is derived from the logistic regression:

$$Logit(P(F)|A(F) > 8500)) = \beta \times [1 + RH + Aspect + USFS]$$

where *Aspect* is the north/south component of aspect computed as $\cos(\pi/2 + \text{aspect} * \pi/180)$ and *USFS* is $log((x + 0.002)/(1 - x + 0.002))$ where x is US Forest Service protection responsibility area as a fraction of total area.

Because the GPD models are assumed to be stationary, $E(A(F)|A(F) < 8500))$ and $E(A(F)|A(F) > 8500))$ are constants. Climate affects expected area burned through its effects on $P(F)$ and $P(F|A(F) > 8500)$, which then determine area burned linearly. Similarly, changes in population affect estimates of $P(F)$ directly, as well as indirectly through the effects of population growth and its spatial footprint on the vegetation fraction, *VEG* (Appendix A.2).

As described in Westerling *et al*. (2011a), future fire probabilities are produced by feeding to the statistical models described above the temperature and precipitation values from downscaled GCM outputs and variables derived from VIC hydrologic simulations forced by downscaled GCM outputs. The methodology used here projects fire–vegetation–climate interactions of present day ecosystems as they are currently managed onto simulated future climates.

3.3. Conditional probability of tract falling within a fire perimeter

Issues of scale and data availability present a significant challenge when it comes to estimating the probability of a given tract being encompassed by fire (the $P(\tau_i \in \tau_F|F)$ of Equation (1)). In reality, this probability is influenced by many factors, such as the location of the tract with respect to vegetation in the region, the location of the tract with respect to boundaries that fire cannot cross, and also induced protective efforts due to value within the tract. Although such factors can be somewhat precisely identified or estimated for near-term risk assessments, we cannot possibly know these relationships for multitudes of tracts decades into the future; therefore, we attempt to bound the impact of such uncertainty.

The basic strategy is to decompose the probability of a given tract falling within a fire perimeter into three components that we can better estimate, confidently bound, or identify as irrelevant. These are the following:

1. $P_0(\tau_i \in \tau_F|\tau_i \in \tau_{VEG})$, the baseline probability a generic vegetated tract will fall within a wildfire perimeter under the assumption that there is nothing of high value to induce greater protection of that tract,
2. $s(V_i)$, a scaling adjustment to the aforementioned probability, to account for value-induced protective efforts that reduce the probability that a given tract will burn, and
3. $P(\tau_i \in \tau_{VEG})$, the probability that a given tract (with associated value V_i) is vegetated and therefore has a nonzero probability of being encompassed by a wildfire.

Note that we have dropped the conditionality on F for convenience, as all equations for the remainder of this section assume a fire event. Using the aforementioned expressions, the probability of a tract burning can be decomposed as follows:

$$P(\tau_i \in \tau_F) = P_0(\tau_i \in \tau_F | \tau_i \in \tau_{VEG}) \times s(V_i) \times P(\tau_i \in \tau_{VEG}) \tag{3}$$

Comprehensive details of our approach are provided in the supplemental material (S1–S9), which includes a complete and integrated description of our methods. Here, we briefly summarize the approach and variables, to provide sufficient context to interpret scenarios and the results.

3.3.1. *Baseline probability of vegetated area burning*

We assume that, prior to adjusting for the existence of valuable structures on a tract, there is a common baseline probability that a given vegetated tract will fall within a wildfire perimeter during a large fire event: $P_0(\tau_i \in \tau_F | \tau_i \in \tau_{VEG})$. That is, given a fire that starts in a hypothetical region covered with some vegetated tracts and some non-vegetated tracts, *all of which have no housing value*, what is the probability that any given vegetated tract will fall within the fire perimeter? Rather than attempt to estimate this probability, we make the assumption that it stays constant across time and scenarios and that it therefore becomes irrelevant when considering relative risk across time periods and scenarios. We argue in the supplemental material [S1] that this assumption is not as heroic as it may fist appear.

3.3.2. *Value-based probability scaling*

We assume that, all else equal, the more housing units there are within a tract of given area, the less likely it is to succumb to wildfire. This is not only due to the physical characteristics of fire spread but also due to the induced protection: Firefighters and managers of wildfire risk may be more likely to direct effort to protecting clusters of many homes, whereas fewer resources may be directed to protecting a lone, difficult-to-access cabin amid many acres of trees. In the limit, large, densely developed areas of land are physically incapable of supporting wildfires and are deemed urban. Together, these dynamics suggest that, at some sufficient level of statistical averaging, the probability that a tract falls within a fire perimeter ($P(\tau_i \in \tau_F)$) should be reasonably modeled as decreasing monotonically as V_i increases, until the tract reaches some threshold density value (which we label the wildland–urban interface [WUI]/ urban threshold), beyond which it is equal to 0. We also treat the WUI/urban density threshold as the threshold beyond which a tract cannot be considered vegetated.

To capture the dynamics described earlier, we further adjust the probability of a tract being within a fire perimeter by a scaling function $s(V_i, D, k, \alpha)$, where D, k, and α are parameters. (We sometimes omit the parameters for convenience when referencing $s(V_i)$). Here, D is the WUI/urban density threshold introduced earlier, α is the area or resolution over which value is considered when evaluating density, and k is a dimensionless shape parameter that controls the concavity of the function as V_i/α varies between 0 and D. While many functions could potentially capture the qualitative relationship, we use the following scaling function for s:

$$s(V_i, D, k, \alpha) = \begin{cases} \left[1 - \left(\dfrac{V_i}{\alpha}\Big/_{D}\right)^k\right]^{\frac{1}{k}} & \text{if } \dfrac{V_i}{\alpha} < D \\ 0 & \text{otherwise} \end{cases} \tag{4}$$

High values of k lead to overall greater exposure (as we define it), in that a rise in value within a tract does not significantly reduce the likelihood of that tract burning until that value nears the WUI/urban threshold, while low values of k (below one) imply that even a little value within the tract induces significant protection efforts.

Later, when discussing the set of model runs we perform, we refer to whether or not we are assuming "protection normalization." When protection normalization is not assumed, the probability of a tract burning always goes down with increasing tract density (according to s), although the overall expected loss within the region may or may not go down depending on the value of the concavity parameter k. Running the model with protection normalization means that total probability of tracts burning is conserved within the region, which we implement by using weights (S2). Therefore, when protection normalization is assumed, the probability of any given tract burning will go up if other tracts in the region gain housing units.

3.3.3. *Scenarios to vary exposure within grid cells*

Here, we are interested in identifying $P(\tau_i \in \tau_{VEG})$, the probability that a given tract (and its associated housing) lies within a vegetated area and is therefore "exposed" to the threat from wildfire. For our long-term scenarios, we know only the distribution of tract values within each region, R, along with the fractions taken up by various land uses. Therefore, to bound the changes in exposure, we would like to consider different scenarios for how housing values in the vulnerable density range are distributed over the vegetated area. This essentially involves specifying the joint distribution of V_i and vegetation status within the grid cell.

We do not attempt to actually estimate this relationship, but instead bound it by considering different cases for the prevalence of vulnerable tracts within the vegetated area of the region. Specifically, we consider a "high-exposure WUI", "low-exposure WUI", and "neutral WUI." The high-exposure WUI assumes housing value is distributed within the region in a way that will produce the greatest expected loss. Because expected loss in a tract is not a monotonic function of the value in that tract (due to the scaling function s), this is not equivalent to assuming the most valuable tracts are in vegetated areas subject to wildfire, because lower density tracts may have a higher expected loss. Intuitively, the low-exposure WUI will produce the lowest (sometimes zero) expected loss, and neutral assumes no correlation between value in tract and vegetation status (excluding urban tracts). These scenarios are formulated in precise mathematical terms in (S3).

3.4. Loss conditional on tract in fire perimeter

The expected damages contingent on a tract falling within a fire perimeter are a function of the value on that land, decreased by a scalar that captures protection efforts at the micro-level—mathematically, expected loss is defined as $L(V_i) := \lambda V_i$. Where V_i is a value expressed in housing units and λ is a scalar that could be a function of tract characteristics, but in our case is assumed constant. (See S4 for discussion about why this is likely to have minimal impact.)

3.5. Calculation of aggregate relative risk

The output of our model lies at the end of a cascading chain of uncertainty, and we do not consider our results to be predictions but rather view this work as exploring the implications of different plausible assumptions about how long-term fire risk is best described. However, we can still take steps to reduce error and increase the validity of our findings by careful consideration of our output measures. In particular, to the extent that our individual model results can be considered a statistical product, we can reduce variance of our results by considering aggregate relative risk at larger spatial scales rather than placing great stock in the absolute outcomes within individual grid cells. Aggregating to larger geographic areas (specifically, the whole state) helps reduce the effects of variance among individual grid cells, because the impact of random error will be reduced relative to our outcomes of interest. To the extent that any systematic bias in our model scales with the magnitude of impacts, the ratio of future losses to present losses evaluated under common assumptions will be a more reliable outcome measure. Most of our results are therefore presented as aggregate statewide relative risk, using common assumptions except where explicitly stated. Specifically, for each combination of scenarios and model uncertainties, we assess the sum of grid cell level expected losses according to the following formula:

$$RR_T = \frac{\sum_j E(LOSS)_{jT}}{\sum_j E(LOSS)_{j0}} \tag{5}$$

where RR is relative risk, j indexes over grid cells within the state, T references two future periods (30 years centered around 2050 and around 2085), and $E(LOSS)$ is defined as in Equation (1). The base period in the denominator references losses simulated for 1961–1990 using climate simulated for 1961–1990 and estimated year 2000 population and vegetation fractions.

While aggregation can be useful, identifying the most appropriate spatial scale to use is actually not a trivial issue, because aggregation is not always better—in particular, it allows the most heavily weighted areas to mask what may be legitimate subregional effects. Therefore, we consider maps that show grid cell spatial patterns, and we show statewide aggregates. We also added some summary statistics for UPlan performance aggregated for the Bay Area and Sierra Foothills as an intermediate level.

3.6. Design of computational experiments

For our study design, we produced two different full factorials of our emissions, climate, and growth scenarios crossed with various parameters designed to explore uncertainties in exposure: one for ICLUS and one for UPlan, as shown in Tables 2 and 3, respectively. In each table, the right two columns identify whether each factor has an influence on the probability of fires (P(F)), or the exposure, or both. Besides being tabularly notated here, they are shown graphically in Figure S2.

A few additional explanations are required for those scenario elements referenced in the Supplement but not discussed earlier.

"Tract Spatial Scale" refers to the fact that the housing density that enters into the scaling function s is most appropriately defined at a particular spatial scale. It is not meaningful at very fine scales such as a few meters, where a structure could easily become engulfed within a wildfire even though the density of that tract is "urban." It is also not meaningful at very large scales, where the density of significant urban areas would just be averaged into the landscape, making it seem like the entire area was vulnerable. Therefore, rather than just assume that the tract-size for our data is most appropriate spatial scale, we also aggregate the ICLUS data to larger spatial scales in order to assess the sensitivity to this assumption. While applied only to the exposure side, we conducted a sensitivity analysis which revealed that in this

Table 2. ICLUS scenarios factorial study design

Variable/scenario	Levels	Affects P(F)	Affects exposure
Emissions scenario	{B1, A2}	X	
Growth scenario	{Low, mid, high}	X	X
Climate model	{NCAR PCM 1, CNRM CM 3.0, GFDL CM 2.1 }	X	
Vegetation allocation method	{Min, neutral, max}	X	X
WUI exposure	{Low, neutral, high}		X
WUI/urban threshold (D)	{147,1000} HH/km^2	X	X
Scaling function concavity parameter (k)	{0.333, 1, 3}		X
Protection normalization	{No, yes}		X
Tract Spatial Scale*	{100, 200, 400, 800} (m)		X

ICLUS, Integrated Climate and Land Use Scenarios.
*This refers to the level at which the density and spatial scale functions are evaluated—essentially the raster size to which the ICLUS data is aggregated. It applies to calculations of housing exposure to wildfire risk only—it does not affect calculations of vegetation fractions.

Table 3. UPlan scenarios factorial study design

Variable/scenario	Levels	Affects P(F)	Affects exposure
Emissions scenario	{B1, A2}	X	
Growth scenario	{Bau, smart, fire}	X	X
Climate model	{ NCAR PCM 1, CNRM CM 3.0, GFDL CM 2.1 }	X	
Vegetation allocation method	{Min, neutral, max}	X	X
WUI exposure	{Low, neutral, high}		X
WUI/urban threshold (D)	{741, 1359} HH/km^2	X	X
Scaling function concavity parameter (k)	{0.333, 1, 3}		X
Protection normalization	{No, yes}		X
Base urban layer	{NLCD, UPlan, CAML}	X	X

Bau, business-as-usual; CAML, California Augmented Multisource Landuse map; CNRM, Centre National de Recherches Météorologiques; GFDL, Geophysical Fluid Dynamics Laboratory; NCAR, National Center for Atmospheric Research; NLCD, National Land Cover Data Base; UPlan, a mixture of NLCD and CAML; WUI, wildland–urban interface.

framework the risk of property loss was relatively insensitive to the effects of tract resolution on vegetation fraction, although the tract spatial scale does play a bigger role in determining exposure.

The "Base Urban Layer" scenario refers to a particular challenge associated with using the UPlan data. It is described in more detail in the supplemental material, but briefly "NLCD," "UPlan," and "CAML" imply different levels urban landcover in the baseline period (applied consistently to the future periods as well). Ex post, we identified that results were not particularly sensitive to this variation, but we did not have an *a priori* ability to assess which was most appropriate.

Lastly, to aid in benchmarking results describing wildfire frequency and burned area, we also estimate scenarios where ICLUS populations and vegetation fractions are held constant at their year 2000 values, in order to see the effects of climate change and the various other parameters independent of population growth. Future work will include additional decomposition to assess driving factors.

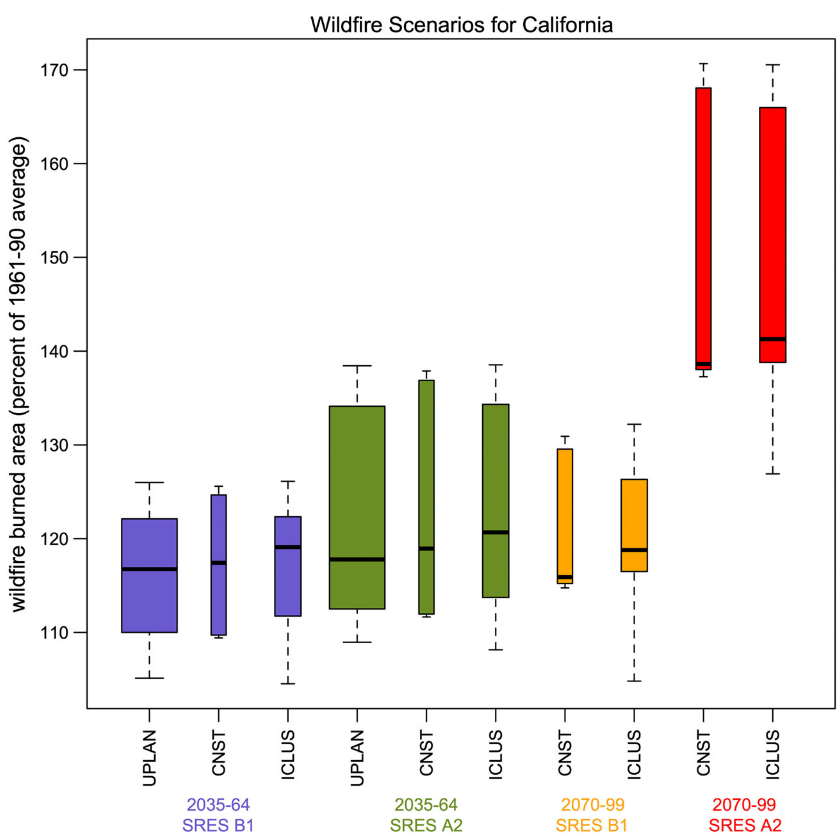

Figure 2. Statewide wildfire burned area scenarios for 2035–2064 and 2070–2099, expressed as a ratio to the average modeled for 1961–1990 (with Year 2000 Population and Land Use). Each UPlan boxplot summarizes 729 scenarios, while each Integrated Climate and Land Use Scenarios (ICLUS) boxplot summarizes 162 scenarios. Constant (CNST) scenarios hold population and footprint constant at year 2000 levels; each CNST boxplot summarizes 54 scenarios

4. RESULTS

As in Westerling *et al*. (2011a), wildfire burned area increases substantially statewide (Figure 2) under the A2 emissions scenarios by end of century. End-of-century B1 emissions scenarios and all mid-century scenarios have similar, lower median increases. Note also that all of the A2 scenarios do pose higher tail risks, with greater spread above the median. This result is driven by the spread of climate model results for the SRES A2 scenario. Burned area in the UPlan and constant population scenarios do not differ appreciably in the statewide totals from the ICLUS scenarios. As in Westerling *et al*. (2011a, not shown), large increases in burned area are for the most part concentrated in forest areas in the Sierra Nevada, southern Cascades, and northern Coast Ranges, with lesser increases in mountain forest areas throughout the rest of the state.

Figure 3 captures the range of results produced by the nearly 35,000 cases considered as part of our experimental design. Unlike Figure 2, which describes changes in area burned, Figure 3 shows the distributions of relative risk (*RR* as described in Equation (5)) in each period of the 21st century, broken out by emissions and growth scenarios for two different housing density thresholds used to define the boundary between vegetated and urban (*D*). The variation associated with each individual box arises from different values for the remainder of our modeling parameters and other assumptions (e.g., scaling parameters, climate model used, vegetation allocation scheme, and WUI exposure scenario). In this figure, each ICLUS box is capturing the variation of 648 individual parameter combinations, and each UPlan box is capturing 486 combinations.

Even though there is a wide variation within many emissions and growth combinations, the figure still identifies several clear trends. First, expected losses of housing units increase in future years under the vast majority of climate and growth scenarios and parameter uncertainty combinations. We can also see that the WUI/urban threshold (*D*) plays an important role in affecting both the magnitude and qualitative nature of the results. High threshold cases are associated with significantly higher relative risk in future periods, with medians between two and three in the 2070–2099 period, although ranging from below one to as high as 10. Low-threshold cases see almost all relative risks between one and two, with a small percentage negative. Qualitatively, high threshold cases follow the trend that scenarios with higher growth produce higher relative risk, while for the low threshold, the higher growth actually may reduce overall risk in some cases. This can be seen in the lower right panel, where the ICLUS high-growth case has a lower distribution than the ICLUS mid case. This can be explained by a combination of two factors: First, a lower threshold implies higher urban development, which implies smaller vegetated areas, which can reduce the probability of large fires. Second, lower thresholds exclude more value being considered exposed, via the value-based scaling function $s(V_i)$.

Figure 3 also provides information about the relative importance of climate and growth scenarios in determining changes in residential wildfire risk, which we explore in more detail in this section. In particular, Figure 3 suggests that, at the state level, variation across growth scenarios is responsible for a greater variation in residential wildfire risk than changes across climate scenarios. This is indeed the case at the state level: A2 scenarios typically lead to greater wildfire risk over B1 scenarios in the 2070–2099 period, but the difference between them is

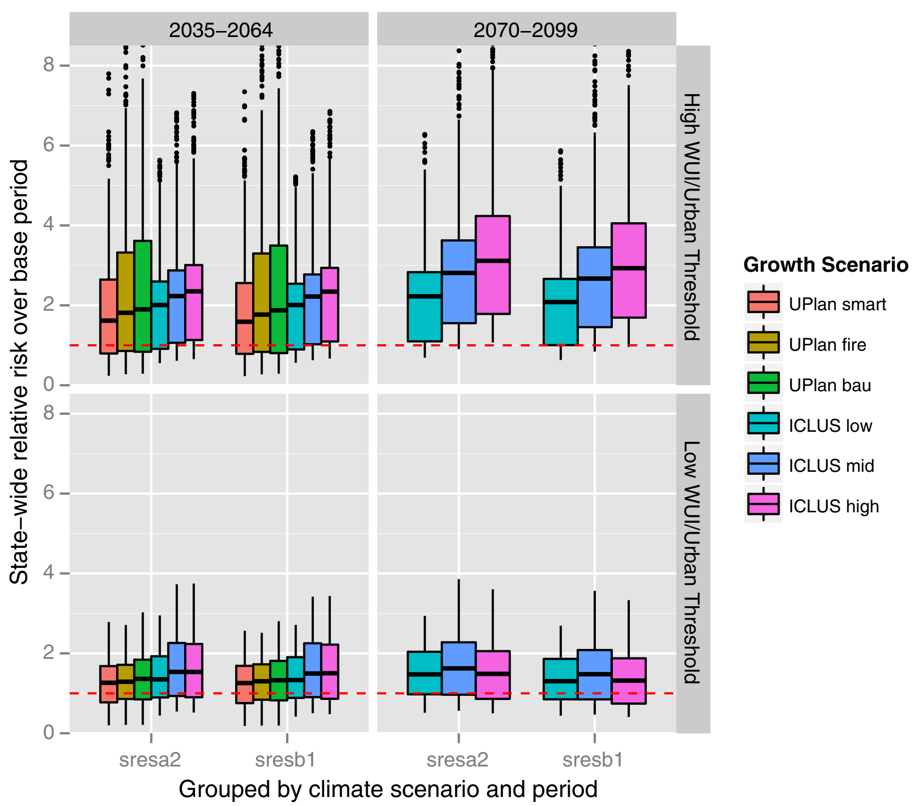

Figure 3. Statewide relative risk by period, broken out by growth scenarios, assumed wildland–urban interface (WUI)/urban thresholds, and climate. Dashed red line represents no change in risk. Notes: 28 Integrated Climate and Land Use Scenarios (ICLUS) and 53 UPlan outliers between 8.5 and 12.09 are not shown; ICLUS and UPlan results capture different parameter assumptions. Vegetation fractions and WUI exposure held at "neutral" for the base year

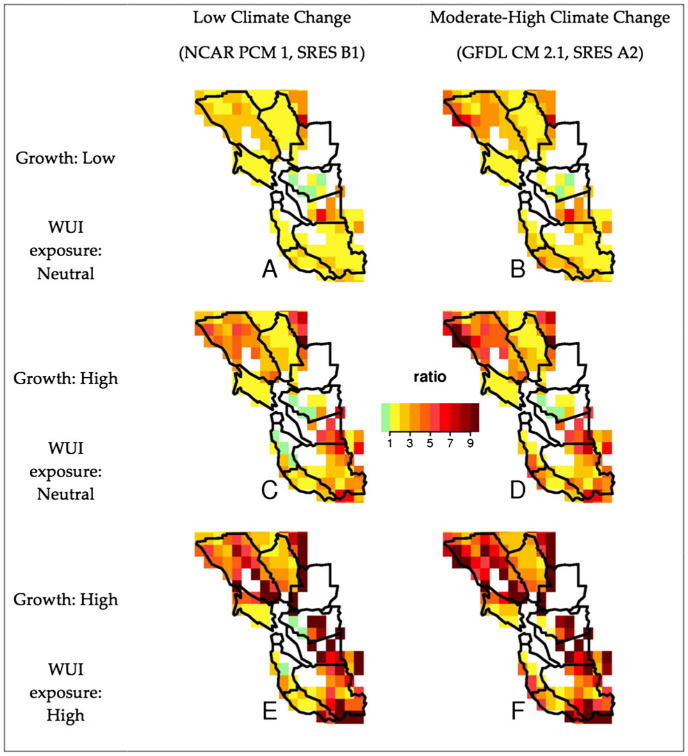

Figure 4. Spatial variation in wildfire risk for the San Francisco Bay Area using the ratio of ICLUS 2070–2099 scenarios to risk estimated for the base period. Six scenarios illustrate the effects of climate change, growth scenario, and wildland–urban interface (WUI) exposure on residential property risk. A relative risk of 1 is equal to no change; therefore, green cells represent reductions in risk. White cells are not modeled. Other parameters are fixed across all six scenarios: WUI/Urban threshold: 1000 HH/km^2, vegetation allocation method (VEG): Neutral, scaling function concavity parameter (k): 0.333, protection normalization: yes, resolution: 100 m

small: 90 percent of cases lead to a relative increase in the range from −1 to 19 percent for A2 relative to B1. By contrast, the corresponding statistics when comparing ICLUS high growth to ICLUS low growth are −24 percent and +72 percent. Note that these are statements about what the impact on risk could be when considering alternative futures rather than parsing out responsibility for future increases in risk between climate and growth. Furthermore, because growth and fire management decisions are made on regional and smaller scales, it is also important to consider regional impacts, which do not necessarily represent statewide trends. We focus on these two aspects next.

4.1. Climate and growth impacts

Figures 4 and 5 show spatial variation in relative residential wildfire risk for the San Francisco Bay and Sierra Foothills under varying climate, growth, and model parameters, comparing end-of-century climate and ICLUS growth scenarios to historical baselines.[8] In each case, the values shown are ratios between expected losses for end-of-century scenarios and corresponding historical baseline scenarios. Growth and WUI exposure scenarios are held constant within each row, while climate scenarios are held constant in each column, with a B1 NCAR PCM1 climate scenario in the left column and an A2 GFDL CM2.1 climate scenario in the right column, and low growth in the first row and high growth in the second row. Thus, moving across columns shows the effect of climate holding everything else constant, while moving across the first two rows shows the effect of growth in the number of households. We can see that in the San Francisco Bay Area, the spatially explicit changes in wildfire risk mirror the larger statewide trends discussed earlier. The impact of climate is noticeable, but a more drastic change can be seen when moving from low growth to high growth. However, looking at the Sierra Foothills, such trends are less clear (Figure 5). In fact, moving from A to B (low-growth/low-climate change to low-growth/moderate-high-climate change) appears to increase risk in many places by as much or more than moving from A to C (low-growth/low-climate to a high-growth/low-climate). Although in both regions, their interaction in D produces the most dramatic changes.

[8]The change between low-climate change and moderate-high climate change bounds the climate scenarios explored here. For a low-climate scenario, a run was used from the NCAR PCM1 model, which is less sensitive to forcing from greenhouse gases, forced with the lower SRES B1 emissions scenario. For the moderate-high climate change scenario, the GFDL CM2.1 model, which is more sensitive to greenhouse gases, was forced with the higher A2 emissions scenario. The term “moderate-high climate change” was used instead of “high climate change” because the warmest scenario explored here does not span the high range of potential scenarios available for California. This terminology is consistent with what has been used for the 2008 California Scenarios Project

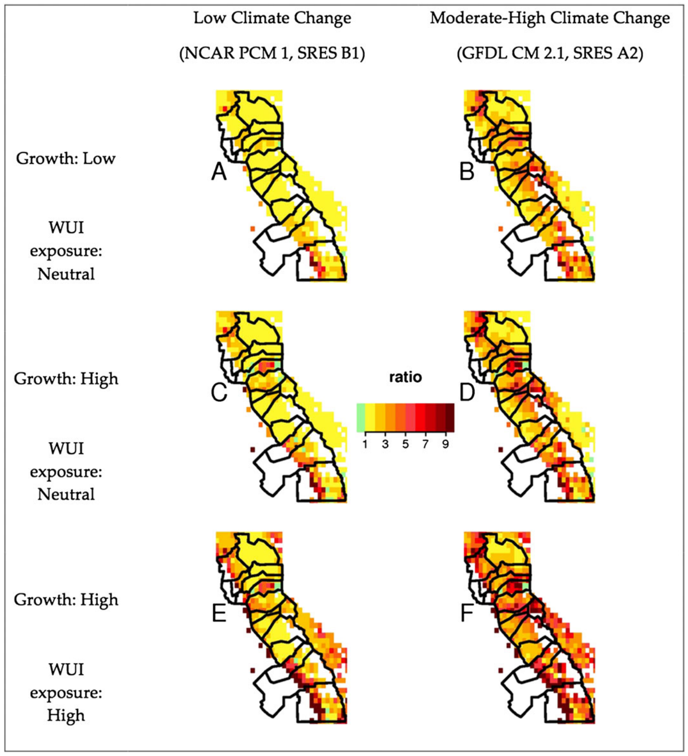

Figure 5. Spatial variation in wildfire risk for the Sierra Foothills using the ratio of ICLUS 2070–2099 growth scenarios to risk estimated for the base period: Six scenarios illustrate the effects of climate change, growth scenario, and WUI exposure on residential property risk. A relative risk of 1 is equal to no change; therefore, green cells represent reductions in risk. White cells are not modeled. Other parameters are fixed across all six scenarios: WUI/Urban threshold: 1000 HH/km^2, vegetation allocation method (VEG): Neutral, scaling function concavity parameter (k): 0.333, protection normalization: yes, resolution: 100 m

4.2. Impact of land use decisions

The first two rows of Figures 4 and 5 illuminate how the relative impact of climate and growth may vary in diverse parts of the state. However, by considering the differences between the second row and the third row, we can see the marginal impact of development decisions on wildfire risk while holding all other parameters constant. Panels E and F describe the same high-growth situation as panels C and D, but consider different WUI housing allocations within each grid cell, with E and F representing cases in which more development occurs at highly exposed density levels within the vegetated areas of the wildland–urban interface. One can see that such a development pattern exacerbates the effects of more extreme climate and growth scenarios. In the Bay Area, the effects of greater high-exposure WUI development are particularly large in eastern Alameda and Santa Clara counties. (See online supplement S10 for a county map of California with relevant counties labeled.) In the foothills on the west side of the Sierra Nevada, these effects are greatest in southern Sierra foothill counties of Madera, Fresno, and Tulare. On the east side of the Sierra Nevada, effects of high-exposure WUI development are particularly notable in Alpine county and northern Mono county under the warmer, drier SRES A2 GFDL CM2.1 scenario (B, D, and F).

The UPlan scenarios for mid-century are able to more clearly illustrate the impact of different growth strategies, because population is held constant across the business-as-usual, smart growth, and fire threat avoidance scenarios. The only change is due to changes in growth patterns across the various UPlan development scenarios. The impact of the changes is summarized in Table 4, which shows how well each UPlan development scenario performed relative to the other scenarios, in the two regions mapped earlier. A few trends emerge: In general, "smart growth" outperforms "fire threat avoidance," which in turn outperforms the "business-as-usual" case. Additionally, the relative impact of each scenario varies notably in both regions. In the San Francisco Bay area, the smart case can reduce expected losses by up to nearly 35 percent, while its strongest effect is less than half that in the Sierra Foothills. We also see that, in the Sierra Foothills, "smart growth" still shows the lowest expected losses, but that the "fire threat avoidance" scenario has many more positive scenarios relative to

Table 4. Pairwise performance of UPlan scenarios for the San Francisco Bay Area and the Sierra Nevada Foothills

Bay Area	% cases with lower risk	Maximum reduction in risk (%)	Maximum increase in risk (%)	Sierra Foothills	% cases with lower risk	Maximum reduction in risk (%)	Maximum increase in risk (%)
Smart vs bau	99.6	34.	0.5	Smart vs bau	100	15.7	NA
Fire vs bau	33.5	2.3	5.3	Fire vs bau	58.3	7.3	2.2
Fire vs smart	0.1	0.4	58.1	Fire vs smart	10.3	1.2	11.6

the San Francisco Bay area. For examples, it outperforms the "business-as-usual" scenario in only about one-third of cases in the Bay Area, while it bests "business-as-usual" cases in 58 percent of scenarios in the Sierra Foothills.

Table 4 supports two conclusions: Land use decisions matter, but the potential consequences of their implementation can (and do) vary across the state. Our model will generally show lower risk for scenarios that place more growth at higher densities, which the smart growth scenario does. However, because our model is highly sensitive to the threshold density, more robust conclusions would require an analysis using scenario data that features more finely resolved density classes, rather than the small number of discrete density classes used in the current UPlan scenarios.

In general, the residential wildfire risk scenarios are imposing a scaled household weighting on projected changes in wildfire. While all scenarios project the greatest increase in the expected area burned by large fires to occur in mountain forests of northern California, the part of the Sierra Nevada that currently is given a high fire threat index by the California Department of Forestry and Fire protection is concentrated in the Sierra foothills, because much of the higher elevations are federal land. This is the same area where we see not only greater increases in risk, both burned area and expected losses, but also a relatively greater effect of the UPlan fire threat avoidance scenarios. It is also unfortunate that the UPlan scenarios do not extend to end of century, because the much larger increases in fire under end of century SRES A2 scenarios would provide a better test of the utility of the fire threat avoidance UPlan scenario.

By contrast, in the wildland–urban interface around the periphery of the San Francisco Bay Area, projected changes in large fire occurrence and burned area are much more modest, while proximity to large population centers guarantees rapid growth in households under the various population growth scenarios. Consequently, the changes in exposure are likely to drive the risk increases, and the density effects of smart growth have a much more noticeable effect.

4.3. Impact of fire risk parameters

From a policy and management perspective, it is important to understand which factors impact risks in qualitatively important ways. In particular, it is the case that under some parameter combinations, higher-growth scenarios lead to a decrease in expected fire losses, while in others, it leads to an increase. What explains the difference?

Figure 6 shows the impact of moving to a high-growth ICLUS scenario from a low-growth ICLUS scenario in 2070–2099, grouped by different combinations of the WUI/urban threshold (D) and the scaling concavity parameter k. In this figure, the y-axis represents the percentage change in 2070–2099 expected losses in a high-growth scenario relative to a low-growth scenario. For example, under the assumption that vulnerability to fire is best described by a low WUI/urban threshold and a small shape parameter ($k = 1/3$), a high-growth scenario is likely to lead to a 20 to 25 percent decrease in statewide expected losses relative to a low-growth scenario. By contrast, for a high threshold and large scaling parameter ($k = 3$), a high-growth scenario would lead to a 50 to 60 percent increase in expected losses.

Figure 6 clearly illustrates that those two parameters alone can determine the sign of the impact. If we think that fire behavior is accurately characterized by a low-threshold and a low-concavity parameter (the lower left), then we can expect a higher-growth scenario to lead to overall lower residential wildfire risk (i.e., paving over the risk), while high values for both imply that a high-growth scenario will lead to a large increase in fire risk. This suggests that, to the extent that the parameters describing exposure to wildfire are exogenous, it is important to learn about their true values in order to understand the impact that different growth scenarios are likely to have. Conversely, to the extent that these values can be affected by management, it provides an estimate of the importance of changing management schemes in ways that are reflected by lower thresholds and scaling parameters. Of course, policy levers in fire management and regional planning are far removed from simply adjusting the parameters of our scaling function. Rather, these are statistical-level descriptors of how the system may reflect different policies.

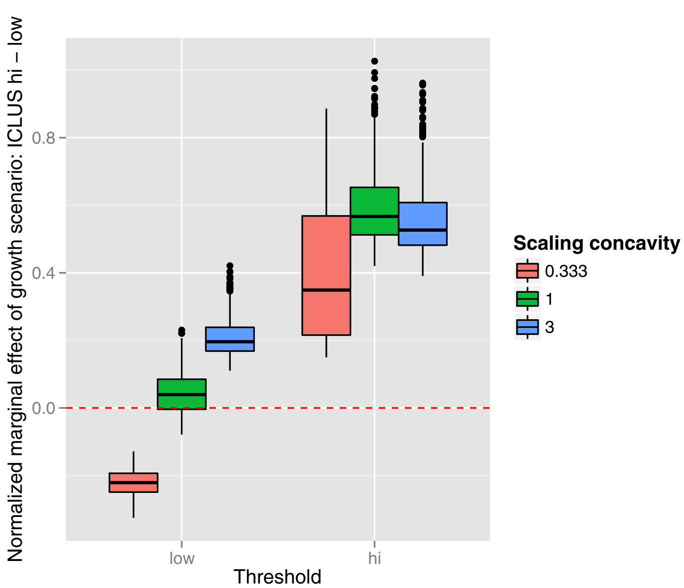

Figure 6. Relative marginal effect of high-growth compared to low-growth scenario in 2070–2099, grouped by different scaling function parameters. The interaction of the two has a strong influence on whether future growth increases or decreases expected losses statewide

4.4. Discussion of uncertainties and caveats

While we go to great lengths to capture variation in outcomes due to different plausible modeling assumptions, there are nevertheless some that remain difficult to account for.

One issue we consider to be of concern is the construction of a fair base period at the grid cell level, because of compatibility of data sources. When we present relative risk compared to the year 2000 development crossed with 1961–1990 climate, our year 2000 data also rely on some modeling assumptions about land use rather than drawing directly from a data set. In particular, our initial vegetation and urban fraction data rely on LDAS information, which was based on imagery collected in the early 1990s. For the maps presented here, we assume that growth happens according to the same rules between the time of LDAS data collection and the year 2000, as it does between LDAS and future years. But this need not be the case in reality. Growth may have proceeded under high-value WUI and high-vegetation-fraction conditions between LDAS and 2000, but could then plausibly shift to a low-value WUI case that also minimizes vegetation fractions in the future. In general, using consistent land use assumptions for the base year and future years not only represent entirely plausible scenarios but also slightly reduces variation in the relative risk. To guard against false precision, our summaries of risk use the common baseline (“neutral” vegetation allocation and WUI exposure). We also emphasize that the ICLUS scenarios do not disaggregate population change and land use change. Future work may explore the disaggregation of these two factors.

Also, for UPlan, the use of a base year mask tends to reduce overall values exposed, and the criteria used to mask out those cells does not correlate perfectly with our WUI/urban threshold criteria that are applied to ICLUS base year data when used with UPlan and that are applied to UPlan in future years. Another factor related to UPlan is that our WUI exposure scheme essentially overrides some of the UPlan modeling at the intra-grid-cell level, which is particularly relevant for assessing the performance of the “fire threat avoidance” scenario. To the extent that relocation of development only shifts UPlan growth patterns within grid cells, our results will not reflect that change—rather, it is only where UPlan’s fire scenario shifts them to grid cells with lower risk as we evaluate it that the change is apparent.

In general, our model makes a variety of assumptions about certain factors remaining constant over space and time, which may impact interpretation of results on both those dimensions. One is that fire probabilities continue to respond to the presence of vegetation and population in the same manner as they have historically. We also assume that the probability of a tract burning conditionally on a fire occurring in the grid cell is independent of the vegetated area of that tract and of the expected size of fires originating in the tract. Perhaps more significantly, we assume that expected losses contingent on a tract falling within a fire do not change over time or space—we devote more discussion to this issue and its relation to policy in the conclusion.

Even where we do explore variation in parameters that lead to different levels of exposure, scenarios apply the same parameters across the state and generally apply parameters consistently across periods. It is theoretically possible that these parameters could vary in ways that exacerbate or mitigate the otherwise risk-increasing impact of new growth. For example, it may be that in areas with high topographic relief, housing remains vulnerable at even higher densities than we have considered, or it may be that communities that are cognizant of their own high fire risk take greater steps to reduce their exposure. Such actions may vary across the state within period, but may also change across periods as well. Either of these could imply that the spatial patterns produced at the level of our 1/8-degree grid cells might not be robust.

5. CONCLUSION

Residential property risk due to wildfire increases over the coming several decades under the vast majority of scenarios that we consider through the end of the century, although high growth can lead to reduced risk under a limited set of parameter combinations. Expected losses increase in almost all scenarios through mid-century, with low WUI/urban thresholds producing changes in risk that commonly range from a 20 percent decrease to a 100 percent increase, while a high urbanization threshold assumption shows many instances in which risk more than triples by mid-century. As a reference point for the magnitude of these changes, from 1990 to 2010, wildfires in state responsibility areas averaged about \$130m of structure damage per year in California (California Department of Forestry and Fire Protection, 2011), which represents only a fraction of the total cost wildfires imposed on the state. It is also important to note that, even in the cases where we show a reduction in expected losses under high growth, that reduction is in part based on an assumption of fire protection response that increases with value—thus lowered expected losses may still be associated with significant increases in other wildfire-related costs.

Increases are due to a combination of climate, population growth, and changing exposure based on how development occurs, while the decreases are due to a combination of reduced vegetated area and reduced exposure because of growth at high densities. Overall, the relative impact of changes in exposure dominates when varying across scenarios considered here. While this is explained in large part by greater changes due to exposure alone, it is also a function of where growth occurs relative to changing climate and wildfire patterns.

Climate change is expected to increase the probability of large wildfires occurring in a substantial portion of the state, but the greatest increases are projected for forests in the mountains and foothills of northern California (Westerling *et al*. 2011a; see also National Research Council 2011; Spracklen *et al*. 2009; Westerling and Bryant 2008). This is largely because climate effects on fuel flammability tend to be important in these forests (Westerling *et al*. 2003; Littell *et al*. 2009). Warmer temperatures are associated with drier conditions and a longer fire season in western US forests, as well as an increased incidence of large forest fires (Westerling *et al*. 2006; Heyerdahl *et al*. 2008; Morgan *et al*. 2008; Littell *et al*. 2009; Swetnam *et al*. 2009; Westerling *et al*. 2011b). In the statistical fire models used here, the probability of large fire occurrence tends to increase with temperature-related increases in summer drought, so the most extreme fire scenarios occur at the end of the century under the higher-emissions scenario examined here (SRES A2), and especially for the model with the greatest temperature sensitivity to the resulting greenhouse gas forcing (GFDL CM2.1) (Westerling *et al*. 2011a).

Integrated Climate and Land Use Scenarios and UPlan growth scenarios tend to concentrate development in and around existing urban areas. These are typically in lower elevation areas with drier climates, where climate effects on fuel availability tend to be more important than on fuel flammability. Temperature is typically less important than antecedent precipitation as a driver of fire in these locations, and consequently, the effects of climate change on fire risks are weaker and less certain than in the less-populated forest areas in northern California forests. As a result, the greatest increases in households in terms of numbers and aggregate values potentially at risk in the state are in areas with weaker and less-certain changes in fire risks. Thus, the effects of growth scenarios tend to dominate those of climate scenarios at the statewide level.

Yet, statewide aggregates tend to obscure interesting details revealed by spatially explicit scenarios for wildfire and property risk. California's ecosystems and fire regimes are quite diverse, and as noted earlier, the greatest increases in wildfire are projected for northern California forests, corresponding to end of century increases on the order of 100 to over 300 percent above the recent historical baseline (Westerling and Bryant 2008; National Research Council 2011; Westerling *et al*. 2011a). Much of this forest area is federal land reserved from residential use, under Park Service and Forest Service management. Growth in households is constrained to occur in private lands in the foothills and small mountain enclaves. In these areas of the state, our modeling indicates that residential property risks are highly sensitive to the growth in the number of households and their spatial footprint, relative to historical baselines. ICLUS scenarios indicate that, by end of century, rapid, sprawling growth in areas on the periphery of the Sierra Nevada could result in substantial increases in residential wildfire risks—with substantial areas projected to increase on the order of five to 10 times above the historical baseline—in a diverse array of communities from Tehama and Butte counties in the far north, to El Dorado, Amador, and Alpine counties in the north, to Madera, Fresno, and Tulare counties in the south (Figure S3). And while patterns in the San Francisco Bay Area tended to more closely reflect parameter and scenario effects at the state level, it is visible from Figure 4 that risk increases vary significantly across the region depending on parameters and scenarios; for example, Panel 4E and 4F show drastic differences in risk along the coastal portion of Sonoma County, and these differences are explained mainly by the different assumptions about the interaction of new development with existing vegetation.

As we have seen, the range of potential outcomes for residential property losses for any given climate and growth scenario is large, suggesting a dominance of inherent uncertainty. Yet the dependency on key parameter values is clear and has implications for policy and research priorities. In particular, the results are largely driven by assumptions about our scaling function $s(V_i,D,k,\alpha)$, which describes how the probability of a tract falling within a fire perimeter varies with the value contained within the tract. This suggests the importance of data collection to characterize this scaling function more accurately, both in its shape and in how it may vary across the state. Doing so will be one step toward more confidently drawing growth and fire management implications using our modeling approach, which currently assumes several factors remain constant throughout the state and over time. At the same time, a very robust result of our scenario analysis is that "smart" growth strategies that concentrate growth in existing urban areas and at higher densities reduced expected losses by mid-century across the vast majority of scenarios.

While varying the parameters of our scaling function clearly revealed their driving role, we note that our analysis does not consider variation in one important parameter: λ, the expected loss contingent on property-specific protective efforts. This variable represents the fraction of value that is lost when a tract is encompassed by wildfire and could be highly variable. To the extent that new housing growth and residential landscaping follows best practices for fireproofing and to the extent that future residents are able to successfully manage their property for greater resilience to fire, future expected losses will be proportionately lower. Indeed, recent state-level policy changes requiring increased defensible space (Public Resources Code 4291) and fire-resistant home construction (California Building Code Chapter 7A) should succeed in lowering this parameter over time in regions of severe fire hazard.

Lastly, from a public policy standpoint, it is also important to consider costs and benefits of growth and land management policy more broadly than just the fire risk context. Besides the important ecological impacts mentioned in the introduction, people build homes with low density in the wildland–urban interface because they perceive it to be a more desirable environment than other alternatives. It is also possible that people may not take all fireproofing steps available to them because they may deem them excessively costly or aesthetically undesirable. To the extent that homeowners may not be fully aware of and may not fully bear wildfire-related risks, there remains a role for government, land management agencies, and private sector actors such as property insurers to improve homeowners' understanding of the risk they bear when making such decisions and to take actions to mitigate that risk.

Acknowledgements

The authors would like to thank Jacquelyn Bjorkman and Jim Thorne for extensive discussion and support in our use of the UPlan scenarios. Alexandra Syphard also provided insights and summary data that helped inform our parameter choices. We are grateful to three anonymous reviewers who provided constructive comments that greatly enhanced readability and clarity of the paper. Funding was provided by the California Energy Commission Public Interest Energy Research Program through the California Climate Change Center and by the National Oceanic and Atmospheric Administration Regional Integrated Sciences and Assessments Program through the California-Nevada Applications Program.

REFERENCES

Allen CD, Savage M, Falk DA, Suckling KF, Swetnam TW, *et al*. 2002. Ecological restoration of southwestern ponderosa pine ecosystems: a broad perspective. Ecological Applications 12(5): 1418–1433.

Bowman DM, Balch JK, Artaxo P, Bond WJ, Carlson JM, Cochrane MA, D'Antonio CM, Defries RS, Doyle JC, Harrison SP, Johnston FH, Keeley JE, Krawchuk MA, Kull CA, Marston JB,Moritz MA, Prentice IC, Roos CI, Scott AC, Swetnam TW, van der Werf GR, Pyne SJ. 2009. Fire in the Earth system, Science 324(5926): 481–484, DOI: 10.1126/science.1163886

Bryant BP, Westerling AL. 2009. Potential Effects of Climate Change on Residential Wildfire Risk in California. Public Interest Energy Research, California Energy Commision: Sacramento, California.

California Board of Forestry. 1996. California Fire Plan. Archived 1996 version available at: http://cdfdata.fire.ca.gov/fire_er/fpp_planning_cafireplan.

California Department of Forestry and Fire Protection. 2011. CAL FIRE jurisdiction fires, acres, dollar damage, and structures destroyed. Fact sheet. http://www.fire.ca.gov/communications/downloads/fact_sheets/firestats.pdf. Accessed October 26, 2011.

Cayan DR, Tyree M, Dettinger M, Hidalgo H, Das T, Maurer E, Bromirski P, Graham N, Flick R. 2009. Climate change scenarios and sea level rise estimates for the California 2009 climate change scenarios assessment. California Energy Commission. Publication number: CEC-500-2009-014-F, 64 pages, August 2009.

Dellasala, DA, Williams JE, Williams CD, Franklin JF. 2004. Beyond smoke and mirrors: a synthesis of fire policy and science. Conservation Biology 18: 976–986.

Gesch DB, Larson KS. 1996. Techniques for development of global 1-kilometer digital elevation models. In *Pecora Thirteen*, *Human Interactions with the Environment - Perspectives from Space*. Sioux Falls, South Dakota, August 20–22, 1996.

Girardin MP, Ali AA, Carcaillet C, Mudelsee M, Drobyshev I, Hely C, Bergeron Y. 2009. Heterogeneous response of circumboreal wildfire risk to climate change since the early 1900s. Global Change Biology 15: 2751–2769, DOI: 10.1111/j.1365-2486.2009.01869.x

Gruell GE. 2001. Fire in Sierra Nevada Forests: A Photographic Interpretation of Ecological Change Since 1849. Mountain Press: Missoula, MT.

Guyette RP, Muzika RM, Dey DC. 2002. Dynamics of an anthropogenic fire regime. Ecosystems 5: 472–486.

Hamlet AF, Lettenmaier DP. 2005. Production of temporally consistent gridded precipitation and temperature fields for the continental US. Journal of Hydrometeorology 6(3): 330–336.

Hansen MC, DeFries RS, Townshend JRG, Sohlberg R. 2000. Global land cover classification at 1 km spatial resolution using a classification tree approach. International Journal of Remote Sensing 21: 1331–1364.

Heyerdahl EK, Morgan P, Riser JP. 2008. Multi-season climate synchronized historical fires in dry forests (1650–1900), northern Rockies, U.S.A. Ecology 89: 705–716.

Holmes TP, Hugget RJ, Westerling AL. 2008. Statistical analysis of large wildfires. Chapter 4 Economics of Forest Disturbance: Wildfires, Storms, and Pests, Vol 79, TP Holmes, JP Prestemon, KL Abt (eds). Forestry Sciences, XIV. Springer: Dordrecht, The Netherlands, 422. ISBN: 978-1-4020-4369-7.

Hurteau MD, Westerling AL, Wiedinmyer C, Bryant BP. 2014. Projected effects of climate and development on California wildfire emissions through 2100. Environmental Science and Technology 48(4): 2298–2304, DOI: 10.1021/es4050133.

Intergovernmental Panel on Climate Change (IPCC). 2000. Special Report on Emissions Scenarios: A Special Report of Working Group III of the Intergovernmental Panel on Climate Change. Cambridge University Press: New York.

Intergovernmental Panel on Climate Change (IPCC). 2007. Climate Change 2007: The Physical Science Basis. IPCC Secretariat: WMO, Geneva.

Johnson EA. 1992. Fire and Vegetation Dynamics. Cambridge University Press: New York.

Keeley JE, Fotheringham CJ. 2003. Impact of past, present, and future fire regimes on North American mediterranean shrublands. In Fire and climatic change in temperate ecosystems of the western Americas, Veblen TT, Baker WL, Montenegro G, Swetnam TW (eds). Springer-Verlag: New York; 218–262.

Kimball JS, Running SW, Nemani R. 1997. An improved method for estimating surface humidity from daily minimum temperature. Agricultural and Forest Meteorology 85: 87–98.

Krawchuk MA, Moritz MA, Parisien M-A, Van Dorn J, Hayhoe K. 2009. Global Pyrogeography: The Current and Future Distribution of Wildfire. PLoS ONE 4(4):e5102, DOI:10.1371/journal.pone.0005102.

Krawchuk MA, Moritz MA. 2011. Constraints on global fire activity vary across a resource gradient. Ecology 92: 121–132.

Lenihan JM. Drapek R, Bachelet D, Neilson RP. 2003. Climate change effects on vegetation distribution, carbon, and fire in California. Ecological Applications 13: 1667–1681, DOI:10.1890/025295.

Liang X, Lettenmaier DP, Wood EF, Burges SJ. 1994. A simple hydrologically based model of land surface water and energy fluxes for general circulation models. Journal of Geophysical Research 99(D7): 14,415–14,428.

Littell, JS, McKenzie D, Peterson DL, Westerling AL. 2009. Climate and ecoprovince fire area burned in western U.S. Ecoprovinces 1916–2003. Ecological Applications 19(4): 1003–1021.

Maurer EP, Wood AW, Adam JC, Lettenmaier DP, Nijssen B. 2002. A long-term hydrologically-based data set of land surface fluxes and states for the conterminous United States. Journal of Climate 15: 3237–3251.

Maurer EP, Hidalgo HG, Das T, Dettinger MD, Cayan DR. 2010. The utility of daily large-scale climate data in the assessment of climate change impacts on daily streamflow in California. Hydrology and Earth System Sciences 14: 1125–1138.

Miller JD, Safford HD, Crimmins M, Thode AE. 2009. Quantitative evidence for increasing forest fire severity in the Sierra Nevada and southern cascade mountains, California and Nevada, USA. Ecosystems 12: 16–32.

Mitchell KE *et al*. 2004. The multi-institution North American Land Data Assimilation System (NLDAS): Utilizing multiple GCIP products and partners in a continental distributed hydrological modeling system. Journal of Geophysical Research 109: D07S90, DOI:10.1029/2003JD003823.

Monteith JL. 1965. Evaporation and the environment. Symposia of the Society for Experimental Biology 19: 205–234.

Morgan P, Heyerdahl EK, Gibson CE. 2008. Multi-season climate synchronized forest fires throughout the 20th century, northern Rockies, U.S.A. Ecology 89: 717–728.

National Research Council. 2011. Climate Stabilization Targets: Emissions, Concentrations, and Impacts over Decades to Millennia. The National Academies Press: Washington, D.C.; 286.

Penman HL. 1948. Natural evaporation from open-water, bare soil, and grass. Proceedings of the Royal Society of London A193(1032): 120–146.

Pierce DW, Westerling AL, Oyler J. 2013. Future humidity trends over the western United States in global climate models and the variable infiltration capacity hydrological modeling system. Hydrology and Earth System Sciences 17(5): 1833–1850.

Preisler HK, Westerling AL. 2007. Statistical model for forecasting monthly large wildfire events in the Western United States. Journal of Applied Meteorology and Climatology 46: 1020–1030.

Preisler HK, Brillinger DR, Burgan RE, Benoit JW. 2004. Probability based models for estimating wildfire risk. International Journal of Wildland Fire 13: 133–142.

Preisler HK, Westerling AL, Gebert KM, Munoz-Arriola F, Holmes TP. 2011. Spatially explicit forecasts of large wildland fire probability and suppression costs for California. International Journal of Wildland Fire 20: 508–517.

Spracklen DV, Mickley LJ, Logan JA, Hudman RC, Yevich R, Flannigan MD, Westerling AL. 2009. Impacts of climate change from 2000 to 2050 on wildfire activity and carbonaceous aerosol concentrations in the western United States. Journal of Geophysical Research 114: D20301.

Stephens SL, Martin RE, Clinton NE. 2007. Prehistoric fire area and emissions from California's forests, woodlands, shrublands, and grasslands. Forest Ecology and Management 251: 205–216.

Stocks BJ, Mason JA, Todd JB, Bosch EM, Wotton BM, Amiro BD, Flannigan MD, Hirsch KG, Logan KA, Martell DL, Skinner WR. 2002. Large forest fires in Canada, 1959–1979. Journal of Geophysical Research 108(D1, 8149): FFR 5-1–FFR 5-12.

Strategic Issues Panel on Fire Suppression Costs. 2004. Large fire suppression costs—strategies for cost management. Available at (April 20, 2007): http://www.fireplan.gov/ resources/2004.html.

Strauss D, Bednar L, Mees R. 1989. Do one percent of the forest fires cause ninety-nine percent of the damage? Forest Science 35: 319–328.

Swetnam TW, Baisan CH, Caprio AC, Brown PM, Touchan R, Anderson RS, Hallett DJ. 2009. Multi-millennial fire history of the giant forest, sequoia national park, California, USA. Fire Ecology 5(3): 120–150, DOI: 10.4996/fireecology.0503120.

Syphard AD, Radeloff VC, Keeley JE, Hawbaker TJ, Clayton MK, Stewart SI, Hammer RB. 2007. Human influence on California fire regimes. Ecological Applications 17: 1388–1402, DOI:10.1890/06-1128.1.

Theobald D. 2005. Landscape patterns of exurban growth in the USA from 1980 to 2020. Ecology and Society 10(1): 32.

Thorne J, Bjorkman J, Roth N. 2012. Urban growth in California: projecting growth in California (2000–2050) under six alternative policy scenarios and assessing impacts to future dispersal corridors, fire threats, and climate-sensitive agriculture. California Energy Commission. Publication number: CEC-500-2012-009.

Thornton PE. Running SW. 1999. An improved algorithm for estimating incident daily solar radiation from measurements of temperature, humidity, and precipitation. Agricultural and Forest Meteorology 93: 211–228.

Verdin KL, Greenlee SK. 1996. Development of continental scale digital elevation models and extraction of hydrographic features. In Proceedings, Third International Conference/Workshop on Integrating GIS and Environmental Modeling, Santa Fe, New Mexico, January 21–26, 1996. National Center for Geographic Information and Analysis: Santa Barbara, California.
Westerling AL. 2010. Wildfires. Chapter 8 in Climate Change Science and Policy, Schneider SH, Mastrandrea MD, Rosencranz A, Kuntz-Duriseti K (eds). Island Press: Washington, DC, USA.
Westerling AL, Bryant BP. 2008. Climate change and wildfire in California. Climatic Change 87: s231–249, DOI:10.1007/s10584-007-9363-z.
Westerling AL, Brown TJ, Gershunov A, Cayan DR, Dettinger MD. 2003. Climate and Wildfire in the Western United States. Bulletin of the American Meteorological Society 84(5): 595–604, DOI: 10.1175/BAMS-84-5-595.
Westerling AL, Hidalgo HG, Cayan DR, Swetnam TW. 2006. Warming and earlier spring increases western U.S. Forest wildfire activity. Science 313: 940–943, DOI:10.1126/science.1128834.
Westerling AL, Bryant BP, Preisler HK, Holmes TP, Hidalgo HG, Das T, Shrestha SR. 2011a. Climate change and growth scenarios for California wildfire. Climatic Change 109(s1): 445–463, DOI 10.1007/s10584-011-0329-9.
Westerling AL. Turner MG, Smithwick EAH, Romme WH, Ryan MG. 2011b. Continued warming could transform Greater Yellowstone fire regimes by mid-21st century. Proceedings of the National Academy of Sciences 108(32): 13165–13170.

SUPPORTING INFORMATION

Additional supporting information may be found in the online version of this article at the publisher's web site.

